



Evolution of electronic and vibrational properties of $M@X_n$ ($M = Ag, Au, X = Ge, Si, n = 10, 12, 14$) clusters: a density functional modeling

Ravi Trivedi^{1,*} and Debashis Bandyopadhyay²

¹Department of Theoretical Physics, Institute Ruder Boskovic, 10000 Zagreb, Croatia

²Department of Physics, Birla Institute of Technology and Science, Pilani, Rajasthan 333031, India

Received: 18 July 2017

Accepted: 4 January 2018

Published online:

1 March 2018

© Springer Science+Business Media, LLC, part of Springer Nature 2018

ABSTRACT

Evolution of electronic and vibrational properties of $M@X_n$ ($M = Ag, Au, X = Ge, Si, n = 10, 12, 14$) nanoclusters is investigated by using first-principle density functional theory (DFT)-based calculations with effective core potentials. To explain the thermodynamic and chemical stability of the ground state cluster in each size, variation of different thermodynamic and chemical parameters, like, binding energy (BE), HOMO–LUMO gap (ΔE), vertical ionization potential (VIP) and vertical electron affinity (VEA) was studied with the variation of the size of the clusters for emphasizing the differences and similarities in the clusters. It is found that Au doping in Ge and Si cages prefers endohedral position, whereas Ag prefers to take the position at the surface of the cages. In addition, IR and Raman spectra of the clusters are also studied to understand the vibrational nature of the stable clusters. At the end, present theoretical results are compared with existing experimental data. Theoretical knowledge of the thermodynamic, chemical and vibrational properties of these specific ground state structures is important for understanding its potential application in the field of optoelectronic science.

Introduction

The explorations of growth mechanism, properties and the insight of stabilities of nanocluster have a long-standing challenge in cluster science. Germanium and silicon are the most significant semiconductor elements in the microelectronic industries. With the ongoing rationalizing of components

toward nanoelectronic devices, there is a significant role of nanosized stable hybrid transition metal-doped semiconductor nanoclusters [1, 2]. A possible move toward the stabilization of Ge and Si nanoclusters is the doping of transition metal (TM) atom as a part of the cage surface or take endohedral position inside the semiconductor cage cluster as found experimentally and theoretically [3–10]. These studies have confirmed that the encapsulation of TM

Address correspondence to E-mail: rtrivedi@irb.hr

atoms leads to stable semiconductor cages. In this direction, Hiura et al. [11] shown that the Si_{12}W hexagonal prism structure is the most stable and it follows 18-electron counting rule in chemistry. In an experimental study, Beck found that addition of third row TM atoms (Cr, Mo, and W) stabilizes the pure Si_{15} and Si_{16} cages [12]. An experimental evidence of high stability of TMSi_{16} (TM = Sc, Ti and V) cluster was established using mass spectroscopy and anion photoelectron spectroscopy by Koyasu et al. [13]. Zhang et al. [14] studied structural and magnetic properties of different endohedral TM metal (TM=V, Cr, Mn, Fe, Co and Ni)-doped silicon clusters. The experimental study of the relative bond strengths between Si–Si and Si–Ag in Si_nAg^+ ($n = 7$ and 10) cluster was reported by Jaeger et al. [15] where they found that photodissociation of Si_nAg^+ cluster proceeds primarily by the loss of metal atoms, and thus indicating Ag–Si bonds in the cluster are weaker than the Si–Si bonds. Chunag et al. [16] studied the Si_nAg ($n = 1$ – 13) cluster by using first-principles investigation and found Ag atom capped exohedral position on the pure Si_n clusters. Ziella et al. [17] carried out computational study of geometries and electronic properties of Si_nAg ($n = 1$ – 15). Recently, Kong et al. [18] investigated the structural evolution and electronic properties of anionic Si_nAg ($n = 3$ – 12) by using anion photoelectron spectroscopy in combination with DFT calculation and found that in these clusters the Ag atom prefers to take exohedral position. Zhao [19] suggested that when a transition metal (TM) is doped into the silicon cluster, the TM atom absorbs the unsaturated bonds present in the semiconductor cluster to form closed shell structures with enhance stability compared to pure silicon clusters. By doping the TM atom(s), one can modify the properties of the hybrid semiconductor cluster in a wide range and it is easy then to tailor the properties of the nanoclusters depending upon the demanding properties [20–22]. A systematic study on the optical properties of TMSi_n (TM = Ti, Cr, Zr, Mo, Ru, Pd, Hf and Os) clusters is reported by the Oliveira et al. [23] which is useful for applications in nanoelectronics. Ma et al. [24] reported the electronic, magnetic and optical properties of TMSi_n (TM = Cu, Ag, Au) cluster where they found that the optical adsorption enhances the doped clusters compared to the pure Si_n clusters. Comparative study on the geometric and energetic properties, absorption spectra and polarizabilities of charged and neutral Cu-doped Si cluster

has been investigated by Lan et al. [25] and found that in the visible range the adsorption spectra are not influenced by a charge of the clusters. The electronic features and chemical bonding of Au-doped Ge clusters are theoretically studied by analyzing the density of states (DOS) and electron localization function (ELF) by Li [26]. Alessandra et al. [27] found that the multiple TM metal doping in isolated interstitial sites in the germanium cages are energetically not favorable. Wu and Su [28] reported the electronic structures and chemical bonding in metal-silicon dimeric monosilicides MSi ($M = 3, 4, 5$ d transition metal elements) in neutral and charged states. Mn-doped germanium clusters (MnGe_n) have been systematically investigated by Zhao et al. [29] using the density functional investigation, and it is reported that the clusters at $n = 5, 9, 12$ and 14 are having higher stability compared to other sizes. Li et al. [30] studied Au–Ge nanocluster and analyzed chemical bonding of some selected stable nanocluster using electron localization function (ELF). Most theoretical investigation [24–30] centered on the stability, magnetic, electronic properties and growth behavior has been done by various group mentioned above, but there is no systematic theoretical report on infrared intensity and Raman activity of Ag- and Au-doped germanium and silicon clusters at different sizes. In this present manuscript, we report a detail study on infrared intensity and Raman activity of Ag-, Au-doped germanium and silicon ground state isomers within the size ranging from $n = 10$ to 14 . The work could be useful to understand the stability and electronic behavior of these clusters which are important for their application as optoelectronic materials. We also hope that these theoretical works would give some light on the experimental characterization of these clusters in future.

Computational method

The search for ground state structures without any imaginary frequencies of cluster was performed by under density functional theory using B3LYP functional [31] as implemented in the Gaussian'03 program package [32]. To completely describe the inner core shell of TM metal atom, we used a double zeta LANL2DZ basis set with effective core potential [33, 34]. To search for low-energy isomers and to see whether Au and Ag atoms prefer endohedral or

exohedral position, a large number of possible initial geometries including one-, two-, and three dimensional configurations are obtained by using the following methods: (1) optimizing the pure Ge_n clusters based on the previously optimized structures [3–5, 7, 35–42] (2) Considering lots of isomeric structures of Ag-, Au-doped germanium by placing Ag, Au at various sites of optimized host Ge_n clusters, i.e., (1) capped (2) encapsulated (3) substituted patterns. All geometries are optimized under no external symmetry constraints. In the report, we present some selected ground state clusters with $n = 10, 12$ and 14 which are our prime focus. Rest of the low-energy isomers in other sizes along with their relative energies are presented in supplementary information (SI Fig. 1). With increasing the size of the clusters, the number of isomers in a particular size increases exponentially. So it is a challenging job to search for a true ground state cluster in a particular size. In our previous report, we have used a global structure predictor method using USPEX (Universal Structure Predictor: Evolutionary Xtalloraphy) and VASP (Vienna AB-initiation simulation package) to get all possible optimized geometric isomers in each size [37]. It is worth to mention here that there are several global search methods are available to predict the geometry of the clusters. Tai and Nguyen [43] adopted a stochastic search method that covers a good number of isomeric structures and increases the chance of finding the ground state geometry. In the present work, we have selected few low-energy geometries based on our previous reports [35, 37] (where we used global structure prediction method) as initial guess geometries with different point group

symmetries and optimized those geometries with different spin multiplicities. In addition, we have examined the harmonic vibration to make sure that each optimized structure is a realistic one (true optimized isomer) without the presence of any imaginary mode of vibration. Further, to examine the optical adsorption characteristic, we performed IR and Raman activity of the clusters.

Results and discussion

To give good reason for the reliability of our method, the vibrational frequency and bond lengths of Ag–Ag, Au–Au, Ge–Ge, Si–Si, Ge–Ag, Ge–Au, Si–Ag and Si–Au dimers are calculated. The calculated results perfectly matched with theoretical and experimental results. We summarized the calculated results and compared with experimental data, which is shown in Table 1. We can wrap up that our calculated results based on B3LYP [31] method and LANL2DZ (ECP) [34, 35] basis sets are very close to the experimental results. So our computational scheme is logically good to depict these clusters.

Structure analysis

In this present calculation, search for ground state energy structures is performed for Ag-, Au-doped Ge and Si cluster with size $n = 10, 12$ and 14 . To find out whether the TM atoms (Ag, Au) will take endohedral or exohedral position, we generated several initial geometries based on the previous report of our

Figure 1 Ground state isomers of TMX_n . (TM = Ag, Au; X = Si, Ge and $n = 10, 12$ and 14).

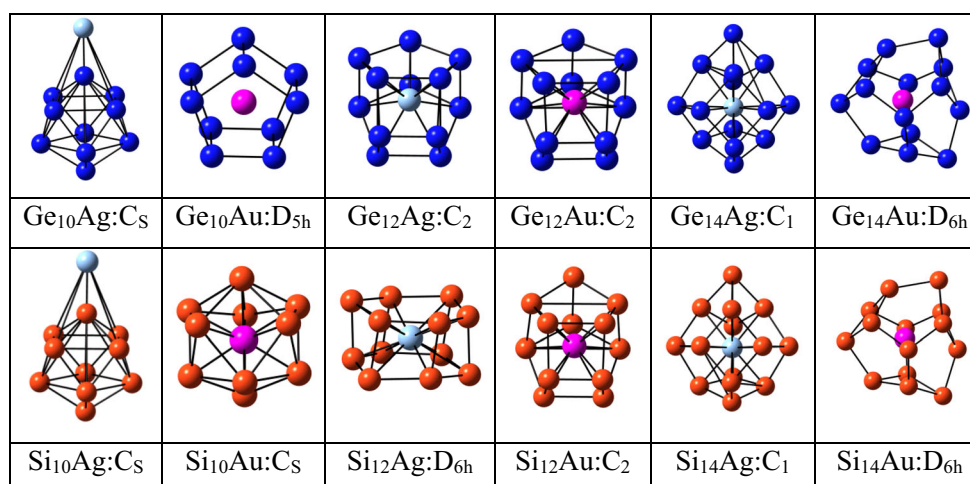


Table 1 Bond distances (Å), lowest frequencies (ω) and IP (eV) of dimmers

Dimers	Bond length	Lowest frequency	IP
Ge ₂	2.44 ^P , 2.36–2.42 [44–46], 2.46 [47]	247 ^a [47]	
Si ₂	2.37 ^P , 2.25 ^a [48]	435.74 ^P , 490 [49]	7.92 ^a [50]
Ag ₂	2.61 ^P , 2.53 ^a [48]	177.218 ^P , 192 [51]	7.59 ^P , 7.56 ^a [52]
Au ₂	2.57 ^P , 2.51 [53] 2.47 ^a [51]	162.49 ^P , 174.00 ^a [54]	9.29 ^P , 9.45 [55]
Ge–Ag	2.56 ^P , 2.55 [56]	184.40 ^P	7.05 ^P
Ge–Au	2.45 ^P , 2.53 [30], 2.38 ^a [57]	207.57 ^P , 249.7 ^a [58]	7.36 ^P
Si–Ag	2.48 ^P , 2.41 ^a [59]	272.35 ^P , 296.9 ^a [59]	7.33 ^P , 7.27 ^a [59]
Si–Au	2.37 ^P , 2.25 ^a [60]	326.47 ^P , 353 ^a [60]	7.68 ^P , 7.42 ^a [60]

a Experimental values, *P* Present calculation

results [3–5, 35] as mentioned before and some other groups [61, 62].

TMGe_{*n*} (TM = Ag and Au; *n* = 10, 12 and 14) clusters

The goal of this present study is looking at relevant features related to the geometric and vibrational properties of the TMGe_{*n*} clusters. For that, we have searched for the ground state clusters in each size and compositions and are presented in the Fig. 1.

For the ground state isomer of AgX₁₀ (X = Si, Ge), we have optimized different endohedral and exohedral doping. We found that bi-capped square antiprism X₁₀ (X = Si, Ge) cage structure with C_s point group symmetry and capped with Au or Ag atom at one of the Si or Ge capping position is the ground state structure as shown in Fig. 1 which is supported by other reported results [28, 63]. However, same AgSi₁₀ structure is found as second nearest neighbor isomer as reported by Guo et al. [64]. For AuX₁₀, structure with Ge and Si is different. AuGe₁₀ ground state structure is a pentagonal prism structure with D_{5h} symmetry and Au atom doped as endohedral atom. The same structure also found as ground state isomer reported is elsewhere [30] using B3LYP/LanL2DZ level of calculations under DFT method, whereas AuSi₁₀ ground state has a point group symmetry C_s which is similar to exohedral Ag-doped Ge₁₀ cage like structure with endohedral Au atom. Very common low-energy isomers of TMX₁₂ isomers are hexagonal prism, icosahedral and fullerene like structures. In the present calculation, we found that AgGe₁₂, AuGe₁₂ and AuSi₁₂ are of similar fullerene type of structure with C₂ point group symmetry, where the TM atoms are doped as

endohedral atom (Fig. 1). However, ground state AgSi₁₂ is a hexagonal prism structure with D_{6h} symmetry. Ground state AgX₁₄ (X = Si, Ge) and AuX₁₄ (X = Si, Ge) are with C₁ and D_{6h} symmetry, respectively, where both Ag and Au atoms are doped inside the X₁₄ (X = Si, Ge) cages. AgX₁₄ (X = Ge, Si) structure is octahedron pyramidal structure, whereas AuGe₁₄ consists of six pentagons and three rhombi, similar to previous works [7, 27, 35, 61].

Electronic properties

Real existence of the clusters mainly depends upon the relative thermodynamic and chemical stabilities of the clusters. In our previous reports [3–7, 35–42], we have presented the effect of the cluster size on their thermodynamic and chemical stability during growth process with the cluster size ranging from 1 to 21. And found that at the beginning stage of the growth process different thermodynamic parameters, like, average binding energy and embedding energy vary rapidly and then saturate. This behavior is due to the thermodynamic instability of the cluster in the smaller size (say, from 1 to 7 depending upon the composition). Other thermodynamic parameters, like, fragmentation energy and second order change in energy fluctuate. Different chemical parameters, HOMO–LUMO gap, ionization potentials (VIP and AIP) and electron affinity (VEA and AEA) are also indication of stability. The variation in these parameters is mainly due to the change in hybridization during growth process. Several other models are also involved to explain the stability of the clusters. Among them electron counting rules [3], shell filled model [65], measure of NICS [66] etc. are important. These need an extensive study with contentious change in the cluster size from 1 to *n* [3–7, 35–42].

With this background, to understand the stability and to evaluate the electronic properties, relative energies of particular stable cluster, the average binding energy, vertical ionization potential (VIP), vertical electron affinity (VEA) and HOMO–LUMO gap are calculated and summarized in Table 2. These energetic parameters are defined as follows:

$$BE = -[E(TM X_n) - nE(X_n) - E(TM)]/(n + 1)$$

$$VIP = -[E(TM X_n)^+ - E(TM X_n)]$$

$$VEA = [E(TM X_n)^- - E(TM X_n)]$$

(X = Ge or Si, TM = Au or Ag and $n = 10, 12$ and 14)

We calculated average binding energy of the cluster as basic parameter which emphasizes on the stability of clusters as shown in Fig. 2. The binding energy values of the clusters are shown in Table 2. The average binding energy of the $AgGe_n$ ($n = 10, 12, 14$) cluster lies in the range of 2.31–2.45 eV, while the range of $AuGe_n$ ($n = 10, 12, 14$) is 2.37–2.50 eV. This indicates that the average binding energy of the clusters increases as the size of clusters increases, and hence, the thermodynamic stability of the cluster increases with the size of the cluster. However, within this small variation in the range of the size of the cluster, (from 10 to 14) it is difficult to make any comment on the thermodynamic stability of the cluster, where the variation in average binding energy value is less than 0.15 eV. The energy difference, (ΔE), between the highest occupied molecular

orbital (HOMO) and lowest unoccupied molecular orbital (LUMO) represents the ability of clusters to participate in a chemical reaction. A large value of HOMO–LUMO gap reflects the higher chemical stability of the cluster and vice versa.

In Table 2, the HOMO–LUMO gap for $Ge_{10}Ag$ is higher than $Ge_{12}Ag$ or $Ge_{14}Ag$. It proves that $Ge_{10}Ag$ cluster is stable in the series. Similarly, VIP and VEA values represent the same result with the value of 6.77 and -2.53 eV. Variation in HOMO–LUMO gap, VIP and VEA all supports the stable nature of X_{10} (X = Ge, Si) size cage doped with Au or Ag.

Similarly, a VIP and VEA value depicts the same result with the value of 6.77 and -2.53 eV. Peak in IP values and minima in EA indicate the nature of stability as shown in our previous results [3, 7]. Similarly, for $Ge_{12}Au$, the value of HOMO–LUMO gap is 1.85 eV, and values for VIP are higher than $Ge_{10}Au$ and $Ge_{14}Au$ which indicates $Ge_{12}Au$ having hexagonal prism-like structure is stable, which is also in agreement with Xiao-Jun Li et al. [30] results. This group suggest the decrease in the tendency of the HOMO–LUMO gap in Ge_nAu cluster along with increasing number of Ge atom. The EA value which is lower in among three also supports our result. If we move toward Si_nAg and Si_nAu ($n = 10, 12, 14$), the binding energy lies in the range of 2.51–2.72 eV for Si_nAg , while 2.57–2.77 eV for Si_nAu clusters.

The HOMO–LUMO gap of $Si_{10}Ag$ shows highest values represent the stability of cluster as shown in Fig. 2. Similarly, highest VIP values 7.71 eV and lowest VEA values -2.42 eV indicate same results that $Si_{10}Ag$ is stable. This result is quite an agreement with the previous theoretical and experimental work [28, 67]. Comparison among Si_nAu ($n = 10, 12, 14$) cluster, $Si_{10}Au$ cluster with highest HOMO–LUMO gap and VIP values indicates that this system is stable as shown in Fig. 2.

IR and Raman analysis

One of the key objectives of this work is to examine the vibrational properties of stable clusters. To check the realistic nature of the clusters, we analyzed the vibrational frequency that is important for us to preliminarily find out some valuable information. These findings are summarized below in the Figs. 3, 4, 5 for TMX_n (TM = Ag, Au; X = Si, Ge; $n = 10, 12$ and 14) clusters via IR and Raman spectra. In order to

Table 2 Average binding energy (BE) (eV), HOMO–LUMO Gap, ΔE (eV), vertical ionization potential (VIP) (eV), and vertical electron affinity (VEA) (eV) of the clusters

Clusters	BE (eV)	ΔE (eV)	VIP (eV)	VEA (eV)
$Ge_{10}Ag$	2.31	2.25	6.77	-2.53
$Ge_{12}Ag$	2.38	1.6	6.79	-2.54
$Ge_{14}Ag$	2.45	1.82	6.95	-2.54
$Ge_{10}Au$	2.37	2.06	6.50	-3.10
$Ge_{12}Au$	2.46	1.85	6.76	-2.40
$Ge_{14}Au$	2.50	1.76	6.68	-2.45
$Si_{10}Ag$	2.51	2.61	7.71	-2.42
$Si_{12}Ag$	2.62	1.82	7.19	-2.66
$Si_{14}Ag$	2.72	1.85	6.94	-2.73
$Si_{10}Au$	2.57	2.28	7.82	-2.58
$Si_{12}Au$	2.68	1.11	6.45	-2.45
$Si_{14}Au$	2.77	1.82	6.87	-2.63

Figure 2 B.E (eV), HOMO–LUMO gap (eV), IP and EA (eV) of the Ag-, Au-doped Ge_n and Si_n clusters ($n = 10, 12,$ and 14).

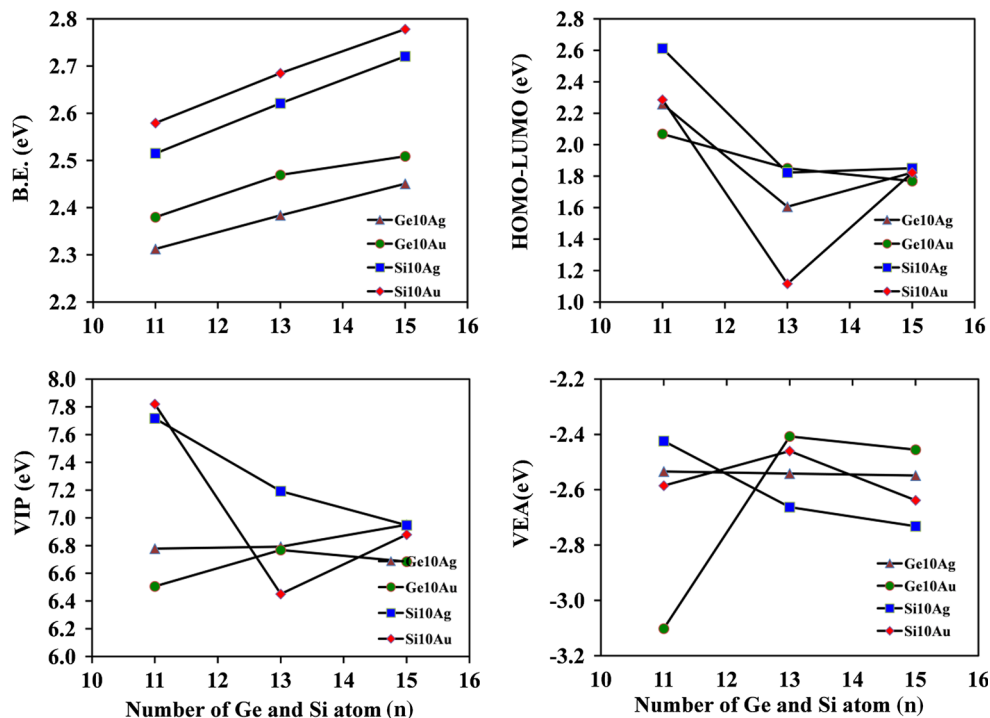
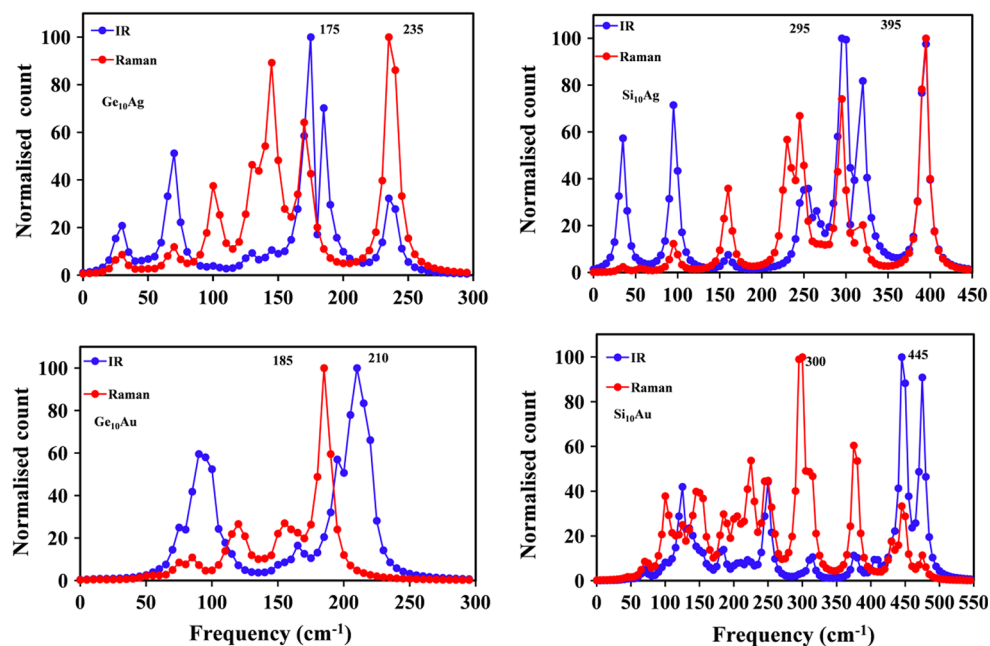


Figure 3 Infrared intensities and Raman activities variation of Ge_{10}Au , Ge_{10}Ag , Si_{10}Au and Si_{10}Ag clusters.



get insight into this work, we compare the IR and Raman results of different same size cluster with different compositions.

The vibrational spectra are unique structural fingerprints of the clusters, and therefore, structural identification is possible experimentally with the theoretical information. We found some prominent differences between the spectra of these clusters

which are due to the different impurities in same cage and vice versa in IR and Raman spectra.

The spectrum of Ag-, Au-doped germanium and silicon clusters shows remarkable differences. As we know that vibration of doped atom always contributes to the IR spectra, while vibration of Si and Ge cages is mainly responsible for Raman activities. Taking impurity as Ag in Ge_{10} and Si_{10} nanoclusters,

Figure 4 Infrared intensities and Raman activities variation of Ge_{12}Au , Ge_{12}Ag , Si_{12}Au and Si_{12}Ag clusters.

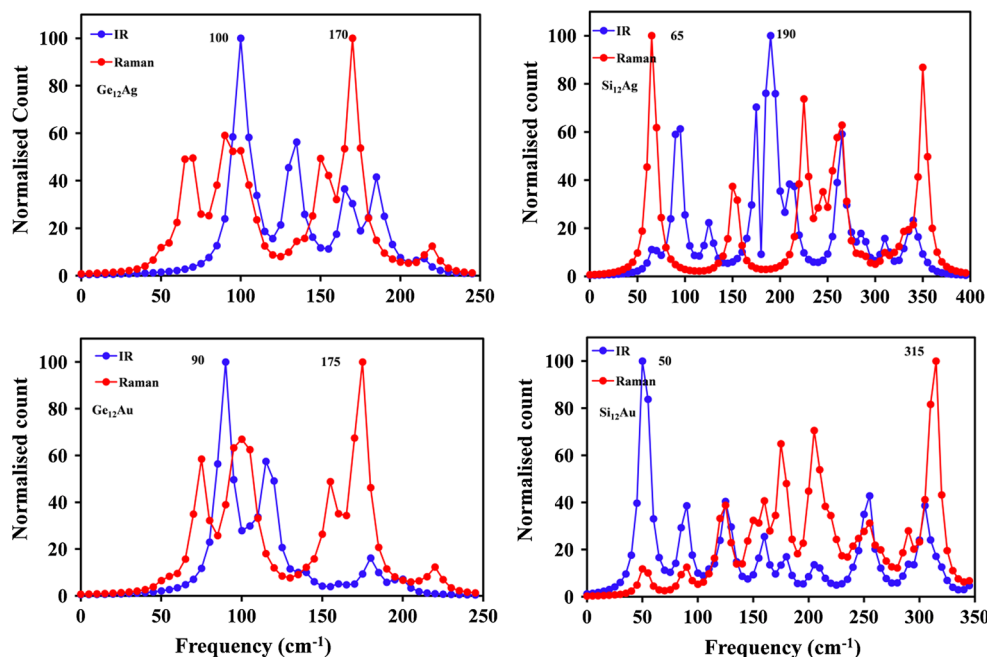
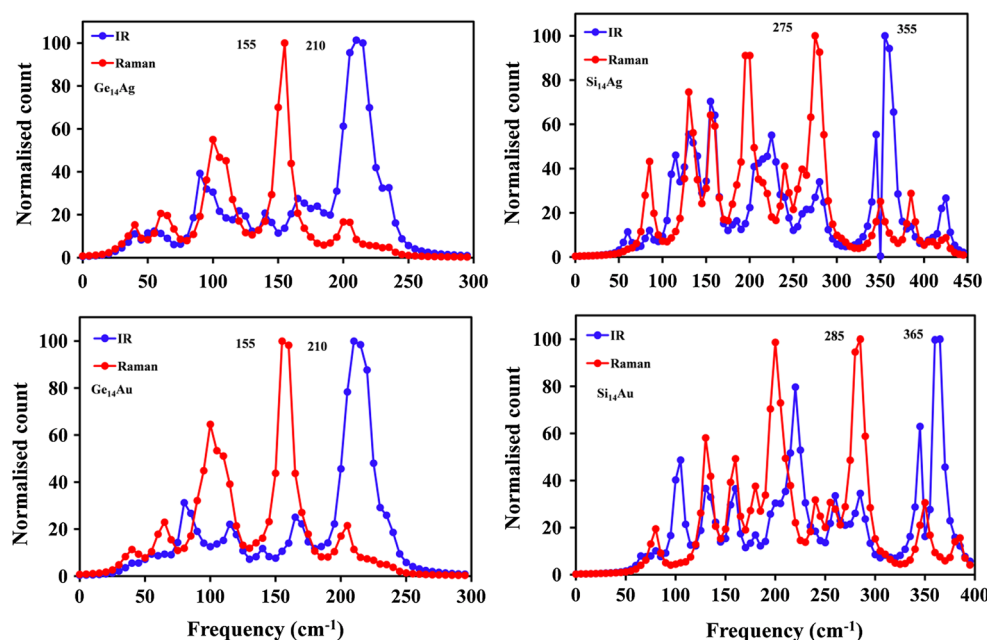


Figure 5 Infrared intensities and Raman activities variation of Ge_{14}Au , Ge_{14}Ag , Si_{14}Au and Si_{14}Ag clusters.



we found the dominating adsorption Raman peak at 235 cm^{-1} for AgGe_{10} , while 175 cm^{-1} for the intensity of IR as shown in Fig. 3. It is quite different for AgSi_{10} system where the dominating peak of Raman spectrum is at 395 cm^{-1} while it is at 295 cm^{-1} for IR. Shifting of peaks toward higher value is an indication of increasing bond strength, indirectly indicating the rigidity of the doped cages. Similarly, the spectrum of IR and Raman for AuGe_{10} indicates a peak at 185 cm^{-1} for Raman, while it is at 210 cm^{-1} for IR,

which nearly agrees with the result obtained by Li [30]. These strongest peaks in IR and Raman are assigned to the stretching of the Ag and Au atoms, respectively, in the Ge_{10} cage. As Cheng et al. [68] suggested in their report that the double degenerate peaks of IR intense predict the antisymmetric stretching of $\text{Si}_2\text{-Si}_6$ and $\text{Si}_1\text{-Si}_3$ bonds and the triple degenerate peaks are associated with stretching vibration of $\text{Si}_2\text{-Si}_1$ bond. We are also getting the same type of double and triple degenerate peaks in

AuGe₁₀ and AuSi₁₀, indicating the presence of antisymmetric vibrational stretching between the Ge–Ge and Si–Si bonds. If we compare with AuSi₁₀, we found a peak at 300 cm⁻¹ for Raman and at 445 cm⁻¹ for IR. The high-frequency peak for AuSi₁₀ reflects its strong bonding nature. So it is worthy to mention here that doping of Au enhances the optical adsorption of silicon cluster than germanium cluster. Ma [24] found the same results for Cu-, Ag- and Au-doped silicon cluster and predicted that the doping of Au in silicon cluster takes stronger adsorption rather than Ag doping which is similar as shown in Fig. 1. This suggests that the doping decreases energy gaps values and improves the transitions of electrons. So comparing our result, it is clear that doping with Au in silicon cage is better than germanium cage for optical properties and for extended optical adsorption. However, a table summarizing all the IR and Raman modes along with their frequency is presented in SI (Supplementary information).

As discussed above, we further calculated IR and Raman for Ge₁₂ and Si₁₂ nanocluster doped with Au, Ag. Figure 4 indicates for Ge₁₂Ag peaks are shifting at 170 cm⁻¹ for Raman and at 100 cm⁻¹ for IR. On the other hand, Ge₁₂Au has a peak at 175 cm⁻¹ for Raman while at 90 cm⁻¹ for IR. Comparing with the Si₁₂Au, we found peak for Raman at 315 and at 50 cm⁻¹ for IR. The maximum Raman activity in clusters assigned to the stretching vibration mode. When we compare Ge₁₂Ag with Si₁₂Ag, we found that peaks are shifting toward higher values as 190 and 65 cm⁻¹ for Raman and IR, respectively. The shifting of IR toward high frequency indicates higher stability. For Si₁₀Ag, the value of IR is 295 cm⁻¹ as pointed out in Fig. 3 and is high as compared with Si₁₂Ag which indicates that Si₁₀Ag is more stable rather than Si₁₂Ag that is in agreement with theoretical [28] and experimental results [67]. There are three and four dominant peaks in Ag-, Au-doped Si₁₀ or Si₁₂ which corresponds to the direction of the motion of doped atom. Ge₁₂Au and Ge₁₂Ag have only one dominant peak due to its high symmetry; however, this is the sum of three nearby frequencies 95, 100 and 105 cm⁻¹. The result of IR and Raman with frequency is quite in agreement with the graph obtained by Xiao Jun Li [30]. Similarly, for Si₁₂Ag, there are several peaks in IR and Raman due to its low symmetric nature, while Si₁₂Au has only one dominant peak for IR and Raman spectra corresponding to breathing mode of the cage. The other

peaks are very small, which may be caused by the causation that these clusters have high symmetry. This result is well consistent with the conclusion obtained by Yejun et al. [69]. Again comparing with these results, we can predict that doping of Ag in silicon will enhance the adsorption rather than in germanium. By investigated results, it is easy to say that doping of Au in silicon is a better option for enhancing adsorption.

Here further we explored the IR and Raman spectra of TM@X₁₄ (TM = Ag, Au; X = Si, Ge) clusters. The theoretical information on IR and Raman modes in the clusters is used to evaluate the molecular structure theoretically and to identify them experimentally. To understand the effect of Ag and Au doping in Ge₁₄ and Si₁₄ cages, we have studied the IR and Raman spectra of all the ground state TM@X₁₄ (TM = Ag, Au; X = Si, Ge) isomers and empty X₁₄ cages. Complete IR and Raman spectra are presented in Fig. 5. Detailed vibrational modes are presented in SI Table 1. Comparing the IR and Raman spectra of Ag- and Au-doped Ge₁₄ clusters, it is found that dominating modes in both the spectrum are nearly identical (SI Table 1). The strongest peaks of IR at 210 cm⁻¹ for both Ge₁₄Ag and Ge₁₄Au, respectively, are the results from the stretching of the Ag and Au atom in the respective cages, whereas the dominate modes in the Raman spectra of Ge₁₄Ag and Ge₁₄Au isomers both correspond to the breathing mode of the cage where all the atoms in the cage vibrate in same phase. Other small peaks are due to the different mode of vibration of the clusters. Similarly, in Si₁₄Au and Si₁₄Ag, the dominate peaks in Raman and IR spectra correspond to the vibration of the cage (breadth mode) and the vibrating of the doped atom is relative to the cage, respectively, as in the other smaller sized clusters. The dominating Raman active frequency is assigned to the stretching vibration of different silicon–silicon bonding in the cluster. The IR and Raman spectra for Si₁₄Ag indicate the IR peaks at 355 cm⁻¹ correspond to the stretching vibration of Ag atom, while Raman peak at 275 cm⁻¹ indicating the breadth mode of the cluster cage. We found many other peaks in IR and Raman spectra due to different types of stretching vibrational mode, such as, antisymmetric stretching, plane stretching, out of plane wagging vibration and breathing vibration mode as reported by Chang et al. [68] for CsSi_n clusters.

With reference to the IR and Raman spectra of AuSi₁₄ and AgSi₁₄ clusters, the dominating peak of the spectra is shifted toward higher frequency side. This is an indication of higher bond strength. However, overall observation indicates that the dominating peak in IR of Au-doped silicon clusters is higher compared to other clusters in the same sizes.

Conclusion

In summary, the structural, electronic and optical properties of TMX_n (TM = Au, Ag; X = Ge, Si; $n = 10, 12$ and 14) have been investigated systematically based on results on IR and Raman activity of the cluster. We found that AuSi_n clusters are stable compared to other compositions studied in each size. It is found that in during the growth process, Au always prefers to take endohedral position both in Si and Ge cages for all sizes, whereas Ag take exohedral position both in Si₁₀ and Ge₁₀ cages. The dominating peaks in IR and Raman are always at higher frequency side in TMSi_n cluster compared to the same transitional doped Ge_n clusters. This tells us that doping of Ag and Au in silicon cages is more preferable to the germanium clusters. It is very interesting that our results obtained by the vibrational spectrum are in good agreement with reported experimental results as discussed. So the structural evolution and vibrational properties of these clusters support the possibility of production of functional materials including nanotubes and nanowires.

Electronic supplementary material: The online version of this article (<https://doi.org/10.1007/s10853-018-2002-4>) contains supplementary material, which is available to authorized users.

References

- [1] Raghvachari K, Logovinsky V (1985) Structure and bonding in small silicon clusters. *Phys Rev Lett* 55:2853–2856
- [2] Brown WL, Freeman RR, Raghvachari K, Schluter M (1987) Covalent group IV atomic clusters. *Science* 235:860–865
- [3] Bandyopadhyay D, Sen P (2010) Density functional investigation of structure and stability of Ge_n and Ge_nNi ($n = 1–20$) clusters: validity of electron counting rule. *J Phys Chem A* 114:1835–1842
- [4] Bandyopadhyay D (2008) A DFT-based study of the electronic structures and properties of cage like metal doped silicon clusters. *J Appl Phys* 104:084308–084317
- [5] Bandyopadhyay D (2009) The study of electronic structures and properties of pure and transition metal doped silicon nanoclusters: a density functional theory approach. *Mol Simul* 35:381–394
- [6] Bandyopadhyay D (2009) Study of pure and doped hydrogenated germanium cages: a density functional investigation. *Nanotechnology* 20:275202–275213
- [7] Dhaka K, Trivedi R, Bandyopadhyay D (2012) Electronic structure and stabilities of Ni-doped germanium nanoclusters: a density functional modeling. *J Mol Model* 19:1473–1488
- [8] Atobe J, Koyasu K, Furusea S, Nakajima A (2012) Anion photoelectron spectroscopy of germanium and tin clusters containing a transition- or lanthanide-metal atom; MGen—($n = 8–20$) and MSnn—($n = 15–17$) ($M = Sc–V, Y–Nb,$ and $Lu–Ta$). *Phys Chem Chem Phys* 14:9403–9410
- [9] Jin Y, Lu S, Hermann A, Kuang X, Zhang C, Lu C, Xu H, Zheng W (2016) Probing the structural evolution of ruthenium doped germanium clusters: photoelectron spectroscopy and density functional theory calculations. *Sci Rep* 6:30116–30124
- [10] Deng XJ, Kong XY, Xu XL, Xu HG (2014) Structural and magnetic properties of CoGe_n ($n = 2–11$) clusters: photoelectron spectroscopy and density functional calculations. *Chem Phys Chem* 15:3987–3993
- [11] Hiura H, Miyazaki T, Kanayama T (2001) Formation of metal encapsulating Si cage clusters. *Phys Rev Lett* 86:1733–1736
- [12] Beck SM (1987) Studies of silicon cluster-metal atom compound formation in a supersonic molecular beam. *J Chem Phys* 87:4233–4234
- [13] Koyasu K, Akutsu M, Mitsui M, Nakajima A (2015) Selective formation of MSi₁₆ ($M = Sc, Ti$ and V). *J Am Chem Soc* 127:4998–4999
- [14] Zhang ZZ, Partoens B, Chnag K, Peeters FM (2008) First principle study of transition metal impurities in Si. *Phys Rev B* 77:155201-1–155201-8
- [15] Jaeger JB, Jaeger TD, Duncan MA (2006) Photodissociation of metal–silicon clusters: encapsulated versus surface-bound metal. *J Phys Chem A* 110:9310–9314
- [16] Lopez del PM, Tiago ML, Chelikowsky JR (2007) Ab initio calculation of temperature effect in the optical response of open shell sodium clusters. *J Chem Phys* 127:144311-1–144311-10
- [17] Ziella DH, Caputo MC, Provasi PF (2011) Study of geometries and electronic properties of AgSi_n clusters using DFT/TB. *Int J Quantum Chem* 111:1680–1693

- [18] Kong X, Deng XJ, Xu HG, Yang Z, Xu XL, Zheng WJ (2013) Photoelectron spectroscopy and density functional calculations of AgSi_n^- ($n = 3\text{--}12$) clusters. *J Chem Phys* 138:244312-1–244312-8
- [19] Ya-Ru Zhao, Kuang XY, Wang SJ, Li FY, Peng L (2011) Equilibrium geometries, stabilities, and electronic properties of the bimetallic Ag_2 -doped Si_n ($n = 1\text{--}11$) clusters: a density-functional investigation. *Zeitschrift für Naturforschung A* 66:353–362
- [20] Koyasu K, Naono Y, Akutsu M, Mitsui M, Nakajima A (2006) *Chem Phys Lett* 422:62–66
- [21] Janssens E, Hou XJ, Nguyen MT, Livenes P (2006) The geometric, electronic, and magnetic properties of $\text{Ag}_5\text{X} + \text{Ag}_5\text{X}$ ($X = \text{Sc, Ti, V, Cr, Mn, Fe, Co, and Ni}$) clusters. *J Chem Phys* 124:184319-1–184319-8
- [22] Zhang M, He LM, Zhao LX, Feng XJ, Luo YH (2009) Tuning magnetic moments by 3d transition-metal-doped Au_6 clusters. *J Phys Chem C* 113:6491–6496
- [23] Oliveria MIA, Rivelino R, Mota FDB, Geurgeuiev GK (2014) surface chemistry of methanol on clean and atomic oxygen pre-covered Au (111). *J Phys Chem C* 118:5501–5509
- [24] Ma W, Chen F (2013) Electronic, magnetic and optical properties of Cu, Ag, Au-doped Si clusters. *J Mol Model* 19:4555–4560
- [25] Lan YZ, Feng YL (2009) Comparative study on the geometric and energetic properties, absorption spectra, and polarizabilities of charged and neutral Cu@Si_n clusters ($n = 9\text{--}14$). *Phys Rev A* 79:033201-1–033201-9
- [26] Li XJ (2013) Theoretical study of Au doped Ge semiconductor clusters. *Adv Mater Sci* 634:2537–2540
- [27] Continenza A, Profeta G, Picozzi S (2007) Transition metal doping in Ge. *J Magn Magn Mater* 310:2147–2149
- [28] Wu ZJ, Su ZM (2006) Electronic structure and chemical bonding in transition metal monosilicides MSi_n ($M = 3d, 4d, 5d$ elements). *J Chem Phys* 124:184306–184320
- [29] Zhao WJ, Wang YX (2008) Geometries, stabilities and magnetic properties of MnGe_n ($n = 2\text{--}16$) clusters: density functional theory investigations. *J Theochem* 901:18–23
- [30] Li X, Su K, Yang X, Song L, Yang L (2013) Size selective effects in the geometry and electronic property of bimetallic Au-Ge nanoclusters. *Comput Theor Chem* 1010:32–37
- [31] Lee C, Yang W, Parr RG (1998) Development of the Colle Salvetti correlation energy formula into a functional of the electron density. *Phys Rev B* 37:785–789
- [32] Hay PJ, Wadt WR (1985) Abinitio effective core potential for molecular calculations potential for the transition metal atoms Sc to Hg. *J Chem Phys* 82:270–283
- [33] Hay PJ, Wadt WR (1985) Abinitio effective core potential for molecular calculations—potential for main group Na to Bi. *J Chem Phys* 82:284–298
- [34] Frish MJ, Trucks GW, Schlegel HB, Scuseria GE, Robb MA, Cheeseman JR, Zakrzewski VG, Montgomery JA Jr., Stratmen RE, Burant JC, Dapprich S, Millam JM, Daniels AD, Kudin KN, Strain MC, Farkas O, Tomasi J, Barone V, Cossi M, Cammi R, Mennucci B, Pomelli C, Adamo C, Clifford S, Ochtrik J, Petersson GA, Ayala PY, Cui Q, Morokuma K, Malick DK, Rabuck AD, Raghavachari K, Foresman JB, Cioslowki J, Ortiz V, Baboul AG, Stefanov BB, Liu B, Liashenko A, Piskorz P, Komaromi I, Laham MAAL, Peng CY, Nanayakkara A, Challacombe M, Gill PMW, Johnson B, Chen W, Wong MW, Andress JL, Gonzalez C, Head Gordon M, Replogle ES, Pople JA (2004) Gaussian 03 revision E 01. Gaussian, Wallingford
- [35] Trivedi R, Dhaka K, Bandyopadhyay D (2014) Study of electronic properties, stabilities and magnetic quenching of molybdenum doped germanium clusters. *RSC Adv* 4:64825–64834
- [36] Dhaka K, Bandyopadhyay D (2016) Magnetism, structures and stabilities of cluster assembled TM@Si_n nanotubes ($\text{TM} = \text{Cr, Mn and Fe}$): a density functional study. *Dalton Trans* 45:12432–12443
- [37] Dhaka K, Bandyopadhyay D (2015) Study of electronic structure, stability and magnetic quenching of CrGe_n ($n = 1\text{--}17$) clusters: a density functional investigation. *RSC Adv* 15:83004–83012
- [38] Trivedi R, Bandyopadhyay D (2015) Hydrogen storage in small size Mg_nCo clusters: a density functional study. *Int J Hydrogen Energy* 40:12727–12735
- [39] Bandyopadhyay D (2012) Architectures, electronic structures, and stabilities of Cu-doped Ge_n clusters: density functional modeling. *J Mol Model* 18:3887–3902
- [40] Kumar M, Bhattacharya N, Bandyopadhyay D (2012) Architectures, electronic structures, and stabilities of TM@Ge_n ($\text{TM} = \text{Ti, Zr and Hf}$; $n = 1\text{--}20$) clusters: a density functional modeling. *J Mol Model* 18:405–418
- [41] Bandyopadhyay D, Kaur P, Sen P (2010) New insight into applicability of electron counting rules in transition metal encapsulating Ge cage clusters. *J Phys Chem A* 114:12986–12991
- [42] Kumar M, Bandyopadhyay D (2008) The electronic structures and properties of transition metal doped silicon nanoclusters: a density functional investigation. *Chem Phys* 353:170–176
- [43] Tai TB, Nguyen MT (2011) A stochastic search for the structures of small germanium clusters and their anions: enhanced stability by spherical aromaticity of the Ge_{10} and Ge_{122-} system. *J Chem Theor Comput* 7:1119–1130

- [44] Islam MS, Ray AK (1988) Many body perturbation theory applied to small germanium clusters. *Chem Phys Lett* 153:496–502
- [45] Northrup NE, Cohen ML (1983) Prediction of bond length and vibrational frequencies of Ge₂. *Chem Phys Lett* 102:440–441
- [46] Pacchioni G (1984) On the ground state properties of the germanium dimer. *Chem Phys Lett* 107:70–71
- [47] Abtew TA, Drabold DA (2007) Ab initio model of amorphous Si_{1-x}Ge_x:h. *Phys Rev B* 75:045201-1–045201-9
- [48] Beutel V, Kramer HG, Bhale GL, Kuhn M, Wayers K, Demtroder W (1993) High resolution isotope selective laser spectroscopy of Ag₂ molecules. *J Chem Phys* 98:2699–2708
- [49] Xiao C, Hagelberg F (2002) Geometric, energetic and bonding properties of neutral and charged copper doped silicon clusters. *Phys Rev B* 66:075425–075447
- [50] Marijnissen A, Meulen JJT (1996) Determination of adiabatic ionization of Si₂ and SiCl by photoionization efficiency spectroscopy. *Chem Phys Lett* 263:803–810
- [51] Herzberg G (1945) Molecular spectra and molecular structure II. Infrared and Raman spectra of polyatomic molecules. Van Nostrand Reinhold, New York, p 632
- [52] Beutel V, Kramer HG, Bhale GL, Kuhn M, Demtroder W (1992) The ionization potential of Ag₂. *Chem Phys Lett* 185:313–318
- [53] Wesendrup R, Hunt T, Schwerdtfeger P (2000) Relativistic coupled clusters calculation for neutral and singly charged Au₃ clusters. *J Chem Phys* 112:9356–9362
- [54] Singh NB, Sarkar U (2015) Geometry, chemical reactivity and raman spectra of gold clusters. *Cogent Chem* 1:1076713–1076729
- [55] Assadollahzadeh B, Schwerdtfeger P (2009) A systematic search for minimum structures of small gold clusters Au_n ($n = 2–20$) and their electronic properties. *J Chem Phys* 131:064306
- [56] Ferrer S, Torrelles X, Etgens VH, Van-der Vegt HA, Fajardo P (1995) Atomic structure of the (4 × 2) surface reconstruction of Ge (001) as determined by X-Ray diffraction. *Phys Rev Lett* 75:1771–1774
- [57] Kingcade JE, Choudhary UV, Gingerich KA (1979) Stability and thermodynamics of ligand-free germanium-gold clusters. *Inorg Chem* 18:3094–3104
- [58] Balasubramaniam K, Liao MZ (1987) CAS-SCF/CI calculations of low-lying states and potential energy surfaces of gold trimer. *J Chem Phys* 86:5587–5590
- [59] Scherer SJJ, Paul JB, Collier CP, Sakally RJ (1995) Cavity ringdown laser absorption spectroscopy and time-of-flight mass spectroscopy of jet-cooled copper silicides. *J Chem Phys* 102:5190–5199
- [60] Scherer SJJ, Paul JB, Collier CP, Keeffe A, Sakally RJ (1995) Cavity ringdown laser absorption spectroscopy and time-of-flight mass spectroscopy of jet-cooled gold silicides. *J Chem Phys* 103:9187–9192
- [61] Jaiswal S, Baber VP, Kumar V (2013) Growth behavior, electronic structure, and vibrational properties of Si_nY anion clusters ($n = 4–20$): metal atom as linker and endohedral dopant. *Phys Rev B* 88:085412–085426
- [62] Kawamura H, Kumar V, Kawazoe Y (2004) Growth, magic behavior, and electronic and vibrational properties of Cr-doped Si clusters. *Phys Rev B* 70:245433–245442
- [63] Li Y, Lyon JT, Woodham AP, Fliecke A, Janssens E (2014) The geometric structure of silver-doped silicon clusters. *Chem Phys Chem* 15:328–336
- [64] Guo P, Ren ZY (2004) structural and electronic properties of TaSi_n ($n = 1–13$) clusters: a relativistic density functional investigation. *J Chem Phys* 121:12265–12275
- [65] Kumar V, Kawazoe Y (2003) Metal-doped magic clusters of Si, Ge, and Sn: the finding of a magnetic superatom. *Appl Phys Lett* 83:2677–2679
- [66] Chen Z, Corminboeuf C, Heine T, Bohmann J, Schleyer PVR (2003) Do all metal antiaromatic clusters exist? *J Am Chem Soc* 125:13930–13931
- [67] Li XJ, Su KH (2009) Structure, stability and electronic property of the gold-doped germanium clusters: AuGe_n ($n = 2–13$). *Theor Chem Acc* 124:345–354
- [68] Luo CG, Jinag HL, Li GQ, Zhang S, Lu C (2016) Theoretical investigation on the geometries and electronic properties of cesium–silicon CsSi_n ($n = 2–12$) clusters. *Struct Chem* 27:457–465
- [69] Yejun L, Jonathan TL, Woodham AP, Lievens P, Fielicke A, Janssens E (2015) structural identification of gold-doped silicon clusters via far-infrared spectroscopy. *J Phys Chem C* 119:10896–10903